Photocatalytic Reactor Design
Guidelines for Kinetic Investigation

Visan, Aura; Van Ommen, J. Ruud; Kreutzer, Michiel T.; Lammertink, Rob G.H.

DOI
10.1021/acs.iecr.9b00381

Publication date
2019

Document Version
Final published version

Published in
Industrial and Engineering Chemistry Research

I&EC research
Industrial & Engineering Chemistry Research

Review

Cite This: Ind. Eng. Chem. Res. 2019, 58, 5349−5357

pubs.acs.org/IECR

Photocatalytic Reactor Design: Guidelines for Kinetic Investigation

Aura Visan,[†] J. Ruud van Ommen,[‡] Michiel T. Kreutzer,[‡] and Rob G. H. Lammertink*[,†]

[†]Soft Matter, Fluidics and Interfaces, MESA+Institute for Nanotechnology, University of Twente, P.O. Box 217, 7500 AE, Enschede, The Netherlands

[‡]Chemical Engineering Department, TU Delft Process Technology Institute, Delft University of Technology, Van der Maasweg 9, 2629 HZ Delft, The Netherlands

ABSTRACT: This review addresses the inconsistencies in interpreting measurements of intrinsic catalyst properties using lab-scale devices. Any experiment must be analyzed in the framework of a model for which the choice and assumptions regarding the necessary parameters must be based on critical reasoning. Physical intuition about the properties of the system is required for both rigorous 3D computational and simplified analytic descriptions. Any divergence between hypothesis and characteristics of the systems affects both the investigation of intrinsic catalytic properties and the later industrial design where parameters are extrapolated outside their obtained operating range. In this work, we make an overview of the underlying physics of photocatalytic reactions, while focusing on pertinent hypothesis, and discuss the consequences for the most basic reactor designs for which guidelines and criteria are provided to meet their premise.

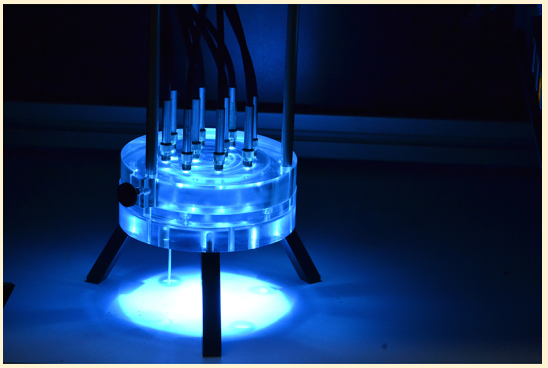

INTRODUCTION

Photocatalysis is still seldom used in industry despite the explosive increase in research efforts.[1,2] There are two research areas that have too little exchange of information and ideas: catalyst fabrication and reactor design. Unfortunately, these disparate contributions do not amount to industrial development if there is not a shared basic knowledge. This paper is aimed at providing a common ground.

Intrinsic kinetics are of paramount importance when developing new catalytic materials. The comparison across different research groups can be possible only if the performance of the catalyst is decoupled from the reactor design. In this way the best approach, for example, to increase quantum efficiency or material resistance can be spotted early on and a more rational trend can follow. It is far too common that research design is motivated by the history of the group or simply left to chance. While diverging toward new ideas has its indisputable value, serendipity has a statistical disadvantage. Purposeful design exerted by a closely interconnected community is the only way to move forward.

Knowledge of the intrinsic properties of a catalyst are essential to optimizing reactor design. This entails not only tuning the mixing rate or superficial velocity according to the mass transfer requirements. The particle density and spatial distribution required to achieve economically feasible conversions define the optical properties of the system, which are necessary for determining the slurry volume for a given light intensity. Moreover, the dynamics of these slurries can alter the particle distribution and affect their aggregation state which impacts their usage of light. These decisions are not as straightforward as maximizing output, but are also affected by operation and material costs, as well as downstream separation. These decisions have to be taken a priori based on an accurate knowledge of the catalytic material, as changing operating conditions may not be sufficient to render the process economically feasible and encourage industrial implementation.

Intrinsic catalyst properties denote values that are independent of reactor design or are explicitly defined inside the operating range for which their validity holds. For example reaction kinetics should be decoupled from mass transfer and light dependency should be accurately described. If simplifications are sought, their applicability regime should be clearly specified. Optical properties for dispersed systems are based on collective particle characteristics, that is, both particle density and aggregation state. Explicit information on the size distribution and the agglomeration development should be given such that the significance of the measurement is not limited to that particular system, but adds to a broader physical intuition that could in the end lead to predictive models.

The objective of this review is to provide guidelines and criteria for the measurement of intrinsic catalyst properties using lab-scale devices and build on the physical intuition for those who are more comfortable with the mathematical description of the phenomena. We start with the dependency of the reaction rate on the local light intensity. Next, we study how to determine the light intensity across the system based

Received: January 21, 2019
Revised: March 18, 2019
Accepted: March 20, 2019
Published: March 20, 2019

DOI: 10.1021/acs.iecr.9b00381
Ind. Eng. Chem. Res. 2019, 58, 5349−5357

on the distribution and properties of the catalytic material. Finally, the mass transfer is analyzed both inside and outside the porous structure. While the first three sections are presented for clarity separately by decoupling their complexity, in the last section we integrate the most important conclusions in an overview regarding reactor design. We address both suspended small photocatalytic particles and wall-coated films of photocatalysts and present the fundamental designs for ideal systems and the deviations that can still be treated analytically. These basic designs can be employed under certain operation conditions for the most commonly used reactors based on the criteria for these approximations.

ELECTRON–HOLE PAIR GENERATION

A photocatalyst is a semiconductor that absorbs photons of equal or higher energy than its band gap which excites electrons from the valence band into the conduction band, leaving positive holes in the valence band of the photocatalyst. The generated electrons and holes can migrate to the surface to engage in redox reactions with adsorbed substrates. This is, however, in competition with electron–hole recombination in the bulk or on the surface of the photocatalyst within a very short time, releasing energy in the form of heat or photons.[3] To maximize the reaction efficiency, recombination should be minimized.

Several ways to reduce electron–hole pair recombination (i.e., enhance the charge separation) via modification of the photocatalysts have been proposed in literature. One is to deposit fine noble metals on the photocatalyst surface.[4,5] While this is an effective approach, one should be aware that such noble metals might also give a catalytic effect in the absence of light, which can obscure experimental results.[6] Another approach is doping the photocatalyst with metal ions. This may both enhance the charge separation and the response in the visible light range, but for some metals (e.g., transition metals) it may also reduce the charge separation.[7,8] Coupling two semiconductors with different band gaps is an alternative way to enhance electron–hole separation.[8] The effect of particle size on recombination is complex: some authors report a reduced charge separation with reducing particle size from 100 to 10 nm,[9] while others report increased charge separation with reducing particle size down to 10 nm.[10] Moreover, the effect of doping on the charge separation can strongly depend on the particle size.[11] A complicating factor is that the crystal phase has an influence on charge separation (anatase versus rutile for TiO_2) but the crystal phase is also influenced by particle size.

The generation and recombination of electron–hole pairs strongly influences the reaction kinetics. There is an ongoing debate about the influence of light intensity and the corresponding regimes. In most photoreactors both regimes coexist: high intensity close to the illumination source and diminishing intensity as light travels through the reactor farther from the source. Thus, a proper kinetic rate expression must take this distribution into account. There are mainly two approaches that we are aware of when deriving the dependency on light intensity, I: the mechanistic approach and the semiconductor physics approach.

In the mechanistic approach a kinetic model is set up based on the law of mass action for both chemical species and electron hole pairs, namely that the rate at which they react is dependent on the diffusion driven collisions which are directly proportional to their concentration. In this case, the recombination rate is defined as $r_{recomb} = k_{recomb}[h^+][e^-]$, where k_{recomb} is the recombination reaction rate constant, $[h^+]$ and $[e^-]$ are the positive and negative charge carrier concentrations. The simplification $r_{recomb} = k_{recomb}[h^+]^2$ can be made for ideal intrinsic semiconductors for which the positive and negative charge carriers are in equal concentration. Intentional or unintentional doping will lead to an excess for one of the carriers. This leads to the proportionality of the photocatalytic reaction rate to $r \propto [h^+] \propto I^{0.5}$ when the consumption of holes due to the chemical reaction is negligible compared to the recombination rate, following the charge carrier governing equation: $I \approx r_{recomb} \approx G$, where G is the generation rate.[12−14] The transition of the exponent from 0.5 to 1 is explained by the competition between electron–hole recombination and photocatalytic reactions.[15−17] Given the very small quantum efficiencies (less than 1%) for these reactions, we find the assumption unreliable.

The semiconductor approach starts also from the charge carriers governing equation using the same assumption regarding the negligible consumption of holes and electrons due to reaction, hence $[h^+][e^-] \approx G/k_{recomb}$. Here, the generation rate dependency on the local light intensity is directly quantified: $G = \alpha\phi/\hbar\omega$, where α is the absorption coefficient, ϕ the photon flux density, and $\hbar\omega$ is the photon energy. Light absorption follows the Lambert–Beer law $\phi(x) = \phi_0 e^{-\alpha x}$. However, the reaction dependency on the electron/hole concentration is extended beyond the mechanism of an elementary reaction. Nielsen et al.[18] follow the electrochemistry reasoning, namely that the driving force for the reaction rate is the photovoltage, V_{ph}, which can be derived based on semiconductor physics:

$$eV_{ph} = k_B T \ln \frac{[h^+][e^-]}{[h^+]_0[e^-]_0} \tag{1}$$

where e is the elementary charge, k_B is the Boltzmann constant, and T is the temperature. Moreover, when the photovoltage drives a rate-limiting electron transfer process, the rate depends exponentially on the photovoltage:

$$r \propto e^{eV_{ph}/k_B T} = \frac{[h^+][e^-]}{[h^+]_0[e^-]_0} \tag{2}$$

which gives in the end the following expression:

$$r \propto \frac{G}{k_{recomb}[h^+]_0[e^-]_0} = \frac{\alpha\phi_0 e^{-\alpha x}}{k_{recomb}[h^+]_0[e^-]_0\hbar\omega} \tag{3}$$

The denominator is a material characteristic, as well as the light absorption coefficient α, which can be measured experimentally using time-resolved microwave photoconductivity via the minority carrier lifetime and the equilibrium hole concentration.[19]

Nielsen et al. do allow for an exponent smaller than 1, $r \propto \left(\frac{[h^+][e^-]}{[h^+]_0[e^-]_0}\right)^{\gamma}$, where γ is the corresponding transfer coefficient for the electron transfer process. The transfer coefficient is a material characteristic related to its morphology which corrects the model for additional phenomena that were not accounted for. One must be aware that the above derivation is valid for ideal intrinsic semiconductors with a homogeneous crystalline lattice. There are multiple phenomena that involuntarily appear in an experimental system such as trap-assisted generation and recombination that arise from

DOI: 10.1021/acs.iecr.9b00381
Ind. Eng. Chem. Res. 2019, 58, 5349−5357

crystalline defects (e.g., unintentional n-doping in TiO_2 due to oxygen vacancies) or impurities. Not to forget, the surface itself is a severe disruption of the periodic crystal.

The transfer coefficient is fundamentally different from the exponent in the mechanistic approach and does not depend on the intensity of light. Nielsen et al. also draws attention on the confusion related to the apparent order in light intensity and shows that also for their system if they simply fit the conversion data to a power law equation, $r_{exp.} = bI_{app}^{\gamma}$ they find a variable, the apparent reaction order γ_{app} that decreases to an asymptotic value for increasing catalyst thickness. This variation in γ_{app} comes from the interplay between reaction rate and diffusion, and therefore, another possible explanation for the experimental findings in literature regarding the variation in the order of light is that for high intensities the reaction rate is fast and diffusion is prevailing, while for low intensities the reaction rate becomes limiting and mass transfer limitations can be neglected. This is also supported in Visan et al. where γ remains 1 for a wide range of light intensities due to the accurate modeling of internal and external mass transport.[20]

RADIATIVE TRANSFER

The propagation of light in heterogeneous (particulate) systems such as photocatalytic slurries is influenced essentially by two processes: elastic scattering and absorption. Scattering represents a redistribution of light in all directions, but usually with different intensities in different directions (anisotropic) depending on the characteristics of the particles such as refractive index, composition, size distribution, morphology and dynamics (change in orientation). Absorption depends on the local light intensity given by the modified electromagnetic field upon light-particle interactions as explained below.

The most general mathematical representation for the total electromagnetic field in the presence of arbitrary particles is given by Maxwell's equations. Solving even for a single particle is not a trivial endeavor.[21] Such computations are important for optical anisotropic particles or for complex geometries and can also provide insight into the effect of neighboring particles. This modeling based on fundamental electromagnetic theory provides light scattering properties for realistic systems.

The relevance for photocatalytic dispersed systems is mostly related to the light intensity distribution which can be solved using the scalar radiative transfer equation (RTE). The derivation of RTE from Maxwell's equations in the far field showing the underlying assumptions is covered by Ripoll.[22] The change in light intensity at every location is solved considering the incoming light that is the light from the source plus the scattered light coming from other particles, and the outgoing light, namely the scattered light contribution of that particular location and the loss due to absorption. Here, the wavelength-dependent light interaction properties, the spectral volumetric absorption and scattering coefficients, α_λ and σ_λ, as well as the scattering phase function, $p(\Omega' \rightarrow \Omega)$, have to be imported to resolve the spectral radiation intensity, $I_{\lambda,\Omega}(s, t)$ reaching a given point $s(x)$ in space and time t, having a given direction of propagation Ω defined by the polar and azimuthal angles, traveling along distances measured by the spatial parameter s.

$$\frac{dI_{\lambda,\Omega}(s,t)}{ds} + \underbrace{\alpha_\lambda(s,t)I_{\lambda,\Omega}(s,t)}_{\text{absorption}} + \underbrace{\sigma_\lambda(s,t)I_{\lambda,\Omega}(s,t)}_{\text{out-scattering}} = \underbrace{j_\lambda^e(s,t)}_{\text{emission}} + \underbrace{\frac{\sigma_\lambda(s,t)}{4\pi}\int_{\Omega'=4\pi} p(\Omega' \rightarrow \Omega)I_{\lambda,\Omega'}(s,t)\,d\Omega'}_{\text{in-scattering}} \quad (4)$$

For the rigorous RTE, isotropic scattering and diffuse reflectance phase functions are usually used.[23−28] The accuracy of the solutions is dictated by simplifications made on the scattering spatial distribution function.[29] For symmetry arguments, the six-flux[30] and two-flux[16,31−33] approximations are utilized the most. The former assumes 3D scattering in the six directions of the Cartesian coordinates, while the latter takes into account only forward and backscattering.

Scattering is always detrimental to the overall energy absorption. Since the scattered light is not lost for the system, but merely contributes to other directions, the change in direction inside the reactor could be intuitively understood as an overall decrease in the optical path. The change in direction inside the reactor will limit the penetration distance accordingly. The change in optical path for different scattering models is illustrated in Figure 1 by the absorbed light fraction,

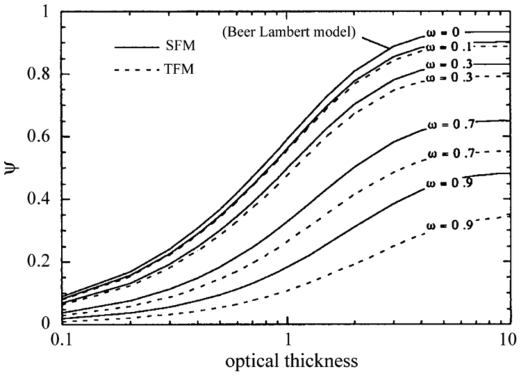

Figure 1. Absorbed light fraction vs optical thickness for different scattering albedos. The dashed lines indicate results predicted by the two-flux model (TFM), while the continuous lines depict the six-flux model (SFM). Figure reproduced with permission from ref 30. Copyright 2007 Elsevier.

Ψ, solved for different scattering albedos, ω, which represents the ratio between the scattering coefficient and the sum of scattering and absorption coefficients. Light absorption is underestimated to the greatest extent in the two flux model due to the highest optical path decrease coming from considering only backscattering.

We argue that a more rational approach should be sought. The coherence between modeling and the properties of the particles is usually missing in the photocatalytic literature. Building a physical intuition is a prerequisite toward understanding the dominant characteristics of each system and provides arguments for simplifying the general RTE. Moreover, intrinsic optical properties, namely the real and imaginary parts of the complex refractive index, n and k, cannot be measured directly, but must be derived from measurable quantities. The measured quantities have to be interpreted in the framework of the RTE model to generate the necessary coefficients.[34−38] In order to fit the measured quantities, external inputs such as the scattering phase function are required.

DOI: 10.1021/acs.iecr.9b00381
Ind. Eng. Chem. Res. 2019, 58, 5349−5357

That is why a good starting point for evaluating the optical properties of individual particles is the scattering angular dependency with the particle size. Useful guidelines are provided by known solutions for Maxwell's equations solved for different limiting cases such as scattering by homogeneous spheres (Mie scattering). The scattering phase function is

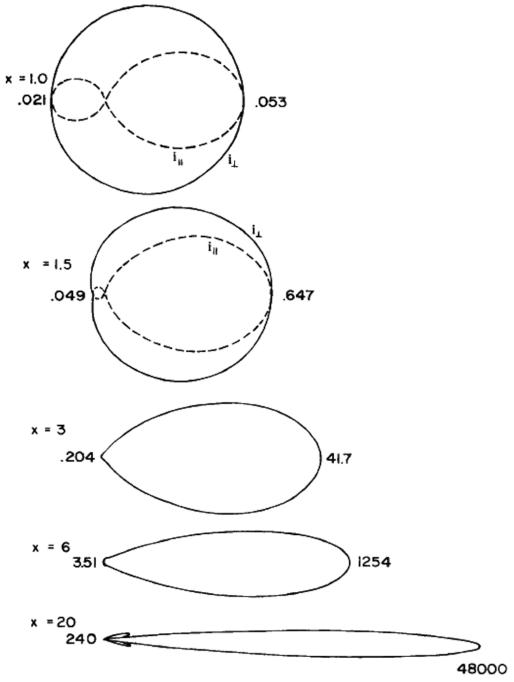

Figure 2. Polar plots of the scattering phase function for different particle sizes with $m_{particle}$ = 1.33 and m_{medium} = 1. Figure reproduced with permission from ref 39. Copyright 2007 Wiley-VCH Verlag GmbH.

illustrated with polar plots in Figure 2 where x is the normalized diameter

$$x = \frac{\pi d m_{medium}}{\nu} \quad (5)$$

where d is the diameter of the particle, m_{medium} is the refractive index of the nonabsorbing surrounding medium and ν is the wavelength. As particles become larger ($x > 3$), isotropic scattering changes to a preferential forward direction.

The scattering magnitude can also be quantified using the scattering cross section which represents the area that would capture the energy of the incident beam equal to the total energy that is scattered in all directions. The corresponding normalized parameter is the scattering efficiency which is equal to the scattering cross section divided by the particle cross section area projected onto a plane perpendicular to the incident beam. The scattering efficiency as a function of particle diameter is illustrated in Figure 3 for TiO_2 particles. Even if the scattering efficiency is presented for 560 nm wavelength due to the visible range interest for the coating industry, a general trend can be noticed. Scattering is negligible for particle sizes much smaller than the wavelength, $x < 0.6$ (0.16 μm in Figure 3), while maximum scattering is achieved when particle sizes approach the wavelength. The scattering efficiency levels off at a value 2 for larger particles, $x > 3$ (0.8 μm in Figure 3), which is characteristic for the geometric

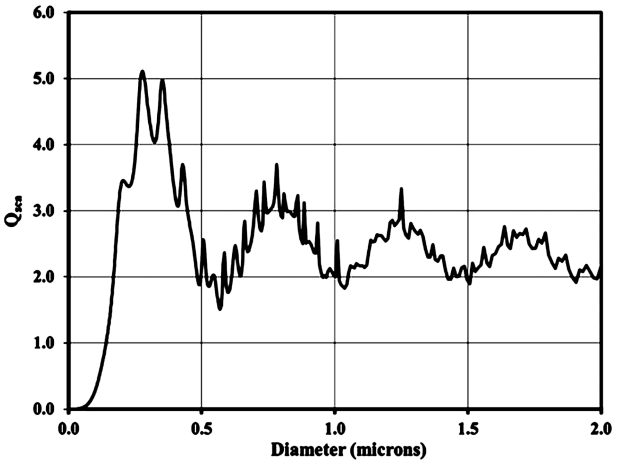

Figure 3. Scattering efficiency vs TiO_2 particle size ($m_{particle}$ = 2.73) embedded in resin (m_{medium} = 1.5) at 560 nm.[40] The ripple structure comes from constructive and destructive interference between incident and forward scattered light. Figure reproduced with permission from ref 40. Copyright 2014 Springer International Publishing.

scattering regime. A general observation is that large particles scatter twice more light than is geometrically incident upon them.

The scattering coefficients selected from literature should correspond to the particle size regime of interest and special care should be given to the radiative transfer model used to extract these optical properties from measurements. A poor choice for external inputs such as the scattering phase function can lead to erroneous coefficients which propagate into further modeling.

Dispersed systems have an inevitable degree of agglomeration. Agglomerate sizes in slurries are above 100 nm; in other words, above the negligible Rayleigh regime. Therefore, the lower particle size range for practical applications corresponds to the highest degree of scattering. Nevertheless, the experimentally observed strong light attenuation for fine particle slurries is still related to the efficient absorption of light by the highly dispersed system. For smaller particles, absorption is always the dominant process due to the higher probability of light−particle interaction. However, larger agglomerates with forward scattering are more prominent in realistic conditions. As aggregation develops, the decrease in absorption is independently accompanied by a decrease in scattering. It is a general misunderstanding that the decrease in absorption is due to enhanced scattering. As the particle size increases, the main reason for lower absorption efficiencies is the shadowing effect. The exponential decay of light inside the particle agglomerate renders smaller internal effectiveness factors[20] (see reactor design section). Most of the light is then absorbed by only the outer agglomerate material.

While the accurate interplay between scattering and absorption is given by rigorously solving the RTE, simplifications can be used under certain conditions. Decoupling scattering and absorption processes can be verified by observing how attenuation scales with particle concentration. If a linear proportionality exists, then the scattering of neighboring particles does not add up to the light reaching every particle. The important implication concerns cumulative scattering. Scattering of individual particles can be summed up due to no interference from neighboring particles, namely

DOI: 10.1021/acs.iecr.9b00381
Ind. Eng. Chem. Res. 2019, 58, 5349−5357

photons are scattered only once. This is a valid assumption for relevant particle concentrations in photocatalysis, which are on the order of a few grams per liter. Crowding effects are noticed only when the distance between particles decreases below 3 times the particle radius.[41] An important consequence is that the exponential profile for attenuation of light is preserved ($\phi(x) = \phi_0 e^{-\beta x}$). Essentially, the scattering coefficient σ and absorption coefficient α can be summed up into an attenuation coefficient β. If this independent absorption hypothesis holds, there are multiple resources that discuss the implications of deviating from ideal systems such as size distribution, various morphologies, or optical anisotropy.[39]

Collimated and diffuse transmittance experiments illustrated in Figure 4 are the standard methods for measuring absorption

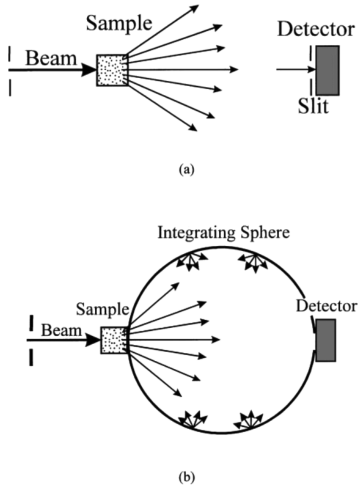

Figure 4. Configurations for measuring absorption and scattering coefficients: (a) collimated transmittance; (b) diffuse transmittance. Figure adapted from ref 24. Copyright 1996 American Chemical Society.

and scattering coefficients. The challenge is that these coefficients cannot be measured independently in slurry systems. Even in the diffusive transmittance mode, the collected light excludes the back scattered light, so it does not amount to a true absorbance measurement. We propose that for particles which are touching, as is the case for immobilized porous layers, scattering can be neglected. If only the near field interaction of a second particle is considered, a significant 20% decrease in scattering is observed.[21] Even if some degree of scattering remains inside the porous film due to consecutive transitions between the two different refractive index mediums, this redistribution of light does not lead to external losses. There is a high probability that it will be captured by the densely packed particle matrix. The high solid volume fraction also ensures a strong absorption which makes the relative contribution of scattering to the total attenuation insignificant.

Given the negligible scattering for immobilize layers, a simple transmittance measurement reveals directly the material absorption coefficient based on the solid volume fraction. This could then be easily translated to the absorption coefficient of the slurry systems for different particle concentrations. An available example in the literature defends our reasoning. The absorption coefficients for immobilized TiO_2 layers has been reported for both dense and porous films. Looking at the 300 nm wavelength, the absorption coefficient in the case of dense layers is between 0.033 and 0.058 1/nm,[42] while for the porous layer with a 0.45 solid fraction the value is 0.023 1/nm.[20] The range for the former study stems from different synthesis conditions which lead to a variation in the crystalline phase composition. If we follow the previous suggestion and normalize the absorption coefficient by the solid volume fraction, the absorption coefficients in the two references become very close, namely 0.06−0.03 versus 0.05 1/nm, revealing its intrinsic value.

MASS TRANSPORT

In chemical reactors, a proper description of the mass transport is crucial to determine limitations and obtain the conversions of reactants and formation of products. In photocatalytic processes, light intensity distribution as well as mass transport can become limiting in terms of the overall conversion. In this section, we will briefly treat the relevant steps in mass transport, starting inside a porous structure, moving to the boundary layer at the surface of the structure and finally to convective transport in the bulk.

Internal Mass Transport. We will first consider the mass transport inside a porous structure. In the framework of this paper, this can be an agglomerate of nanoparticles in a slurry system or a porous immobilized catalyst layer. This internal mass transport is governed by diffusion and reaction only at given x:

$$D_{\text{eff}}\frac{\partial^2 c}{\partial y^2} - r = 0 \tag{6}$$

with the following boundary conditions for a slab geometry. At $y = -\delta$, $D_{\text{eff}}\frac{\partial c}{\partial y} = 0$ and at $y = 0$, $c = c_s$, where r is the reaction rate, $D_{\text{eff}} = D\frac{\epsilon}{\tau}$ is the effective diffusion coefficient, D is the molecular diffusion coefficient, ϵ is the porosity, τ is the tortuosity and δ is the catalyst thickness.

The equation can be solved analytically for a first-order reaction rate $r = kc$, where k is the rate constant. This is an effective bulk reaction rate often assumed for simplicity, representing the surface reactions taking place inside the porous material. The concentration profile and the net reaction rate (inward flux) are

$$c(y) = c_s\frac{\cosh(\phi(1 + y/\delta)}{\cosh(\phi)} \tag{7}$$

$$N_{y=0} = D_{\text{eff}}\frac{\partial c}{\partial y} = c_s\frac{D_{\text{eff}}}{\delta}\phi \tanh\phi \tag{8}$$

where c_s is the surface concentration at the particle-liquid interface. It is important to realize that this surface concentration can be different from the bulk in case external mass transfer limitations are present, as will be discussed later.

The dominating mechanism can be evaluated using the Thiele modulus ϕ and the internal effectiveness factor η defined in Table 1 for a first order reaction rate. The former computes the ratio between the reaction and the diffusion time scales, while the latter gives the ratio between the net reaction rate and the surface reaction rate, namely the rate in the absence of concentration gradients.

Weisz and Prater established that $\phi \leq 10^{-1}$ to neglect or avoid concentration gradients ($\lesssim$5% deviation from a flat concentration profile). The formal criterion[43] for a first order reaction is

DOI: 10.1021/acs.iecr.9b00381
Ind. Eng. Chem. Res. 2019, 58, 5349−5357

Table 1. Performance Parameters

geometry	Thiele modulus	internal effectiveness factor
slab	$\phi = \sqrt{\frac{k}{D_{\text{eff}}}}\delta$	$\eta = \frac{\tanh\phi}{\phi}$
spherical	$\phi = \sqrt{\frac{k}{D_{\text{eff}}}}R_p$	$\eta = \frac{3}{\phi^2}(\phi\coth\phi - 1)$

$$\frac{r_{\text{net}}R_p^2}{c_s D_{\text{eff}}} < 0.6 \tag{9}$$

where r_{net} is the net or observed reaction rate. An even more practical meaning is conveyed by the internal effectiveness factor, which directly expresses the fraction of the catalyst that is being utilized. Thiele modulus and internal effectiveness factor are also derived for reaction rates taking into account their dependency on the local light intensity. For clarity, these will be presented in the reactor design section.

External Mass Transport. The reaction−diffusion equation can be solved for boundary conditions that specify the concentration at the catalyst surface which can be determined only if external transport is known. Equality between the surface and bulk concentrations implies perfect mixing, but even in a well-stirred volume this is typically not reached for fast catalytic conversions: depletion of reactants at the catalyst surface is still taking place. The easiest method to incorporate this additional resistance to mass transport is to use a stagnant boundary layer model which connects the bulk concentration to the surface concentration via the mass transfer coefficient, k_m. The flux continuity boundary condition is

$$N_{y=0} = k_m(c_b - c_s) = r_{\text{net}}\delta \tag{10}$$

This flux continuity matches the mass transport through the boundary layer to the total conversion inside the porous catalyst. Using the definition of the internal effectiveness factor, $r_{\text{net}} = r_s\eta = kc_s\eta$, and solving the equation for the unknown surface concentration, the net reaction rate becomes

$$r_{\text{net}} = \frac{\eta k c_b}{1 + (\phi\tanh\phi)/Bi_{\text{m}}} \tag{11}$$

where the mass Biot number evaluates the ratio between the internal and external mass transport coefficients, $Bi_{\text{m}} = \frac{k_{\text{m}}}{D_{\text{eff}}}\delta$. A straightforward criterion for assessing the effect of external transport on the reaction rate was introduced by Carberry.[44] For

$$\frac{\eta k}{k_{\text{m}}A} < 0.1 \tag{12}$$

the reaction rate constant derived from the observed reaction rate reaches its intrinsic value, where A is the external surface to volume ratio (1/m). The mass transfer coefficient depends on velocity and can be determined experimentally with the benzoic acid dissolution method[45] or can be computed via empirical correlations:[46] $Sh = f(Sc, Re)$ with $Sh = \frac{k_{\text{m}}d_{\text{p}}}{D}$, $Sc = \frac{\nu}{D}$, $Re = \frac{\overline{u}d_{\text{p}}}{\nu}$, where ν is the kinematic viscosity, d_{p} is the diameter of the particle agglomerates and $\overline{u}$ is the superficial velocity of the fluid. Welty and Wicks[47] give a comprehensive list of convective mass transfer correlations for various types of reactors and operating conditions.

Convective Transport. Until now, we have worked under the assumption of a constant bulk concentration. However, the replenishment of the bulk solution is not instantaneous and needs to be accounted for a temporal and/or spatial development of the bulk concentration. The concentration in the bulk of the reactor is determined by the velocity profile, which influences both the residence time distribution as well as the mass transfer capacity. Following the general approach of the paper, we will seek to simplify the daunting transient 3D analysis to a 1D model. The most basic reactor design is the plug flow model, assuming zero axial dispersion and infinite radial dispersion. The velocity is assumed constant along the axial direction, resulting in

$$u\frac{\partial c_b}{\partial x} = r \tag{13}$$

where c_{b} depends only on x since the radial concentration gradients are localized within the boundary layer. Lumping both internal and external mass transport limitations into an apparent reaction constant k_{app}:

$$k_{\text{app}} = \frac{\eta}{1 + (\phi\tanh\phi)/Bi_{\text{m}}}k \tag{14}$$

c_{b} has the well-known expression: $c_{\text{b}} = c_0\, e^{-k_{app}\cdot x/u}$.

This model is equivalent to an ideally stirred batch reactor where the position along the plug flow reactor correspond to a residence time, $\frac{x}{u} = t$.

The plug flow reactor (PFR) is relevant in practice for a continuous operation of a slurry reactor or an effectively mixed immobilized reactor. Concentration gradients can be accounted for by using deviations from plug flow. The axial dispersion approximation can be used to evaluate molecular and turbulent mixing:

$$D_{\text{a}}\frac{\partial^2 c_{\text{b}}}{\partial x^2} - u\frac{\partial c_{\text{b}}}{\partial x} = r \tag{15}$$

where the axial dispersion coefficient D_{a} can be experimentally determined from residence time distribution measurements[43] or derived using empirical correlations. Fortunately, eq 15 has analytical solutions for zeroth and first order reaction rates. Using the first order reaction rate model in eq 11 gives the following c_{b} profile:

$$c_{\text{b}} = c_0\frac{4\sqrt{1 + \frac{4Da_I}{Pe}}\exp\left(Pe/2\left(1 - \sqrt{1 + \frac{4Da_I}{Pe}}\right)\right)}{\left(1 + \sqrt{1 + \frac{4Da_I}{Pe}}\right)^2 - \left(1 - \sqrt{1 + \frac{4Da_I}{Pe}}\right)^2\exp\left(-Pe\sqrt{1 + \frac{4Da_I}{Pe}}\right)} \tag{16}$$

where the Péclet number is $Pe = \frac{\overline{u}x}{D_a}$ and the first Damköhler number is $Da_I = \frac{k_{\text{app}}x}{\overline{u}}$ with $\overline{u}$ being the average velocity. The axial dispersion model can be used only for $Pe > 20$.[48]

REACTOR DESIGN AND OPERATION

In the last section, we discuss the underlying assumptions of basic reactor designs and provide criteria that ensure these conditions are accurately met in practice. Here, we integrate the analysis of the physical phenomena presented separately in the first three sections.

Dispersed Systems. Slurry reactors are widely used in photocatalysis. Such reactors are obtained by dispersing photocatalyst nanoparticles in aqueous environments. These

DOI: 10.1021/acs.iecr.9b00381
Ind. Eng. Chem. Res. 2019, 58, 5349−5357

particles are often already aggregated because of their production process (e.g., combustion synthesis for TiO_2 P25), and agglomerate even further to larger clusters. These agglomerates typically have a size in the order of 1 μm[24,49] and a very open structure. To verify if internal mass transfer can be ignored, a sample from the catalyst aggregates could be redispersed for instance using ball milling. The conversion under identical conditions should be similar before and after crushing. To work under the assumption of an ideally stirred system, the mixing rate should be increased until no further change in conversion is noticed. In this case, external mass transfer can also be ignored, and a homogeneous concentration of reactants and products throughout the system can be assumed. Another type of dispersed system is the stagnant slurry reactor. Here, in the absence of convection, the underlying physics encompass diffusion and reaction only, such that the mathematical description resembles the immobilized catalyst case.

When designing a photocatalytic slurry reactor for optimum determination of reaction rates, one wants to have a nearly constant light intensity inside the catalyst agglomerate and throughout the reactor. The criterion for neglecting light dependency is defined as the decay length in Visan et al.[20] for more than $1/e$ transmission corresponding to $\delta < \frac{1}{\alpha}$ and in Motegh et al.[16] for less than 5% deviation of photoreaction rate per particle from the maximum photoreaction rate in the absence of shielding, corresponding to $\delta < \frac{0.1}{\alpha}$. To illustrate the concept, a TiO_2 layer with a porosity of 0.45 has a characteristic decay length for the light intensity of ~1 μm.[20] In a single agglomerate of ~1 μm the porosity is much higher, thus it is reasonable to assume a constant light intensity within the agglomerate: that is, each individual particle is equally exposed to the light.

A more general criterion that takes into account multiple scattering is that for common values of the scattering albedo (around 0.7), one has to work at an optical thickness below 0.2 to be able to volume-average the reaction rate.[16] When designing a photocatalytic slurry reactor for maximized use of photons, the optical thickness should be at least 3.5 for low photon fluxes or 6.5 for high photon fluxes. In that case less than 5% of the photons leave the reactor unused.[16] These threshold values are only a weak function of the scattering albedo.

The guidelines above are for two-phase systems: fine particles dispersed in a liquid. However, Motegh and co-workers[33] showed that the same guidelines can be used for slurry reactors with gas bubbles, that is, three-phase systems. For a gas fraction below 20% and bubble diameters around 3 mm, typical values in such reactors, the effect of the additional scattering by the bubbles on the photoreactor performance is insignificant, and the same limiting values for optimal thickness apply.

Immobilized Systems. There is a general preference for dispersed catalytic systems due to their enhanced mass transport capacity, as the small interparticle distance ensures a small diffusion length scale. However, the additional separation step and the corresponding complexity for continuous operation motivate the use of immobilized systems. Moreover, slurry systems have inherently lower quantum efficiencies, as various degrees of scattering are unavoidable.

The general approach for preserving high mass transfer rates for immobilized systems is either to operate at high flow rates which generates strong turbulence, being aided sometimes by static mixers, or reactor design for sudden changes in flow direction or to maintain a small diffusion length scale by decreasing the transverse dimension of the flow channel. In cases in which mass transport in the liquid is affecting the conversion, quantification of this transport is required in order to obtain intrinsic kinetics for the catalytic conversion.

The former case, namely the well-mixed reactor with immobilized layer can be modeled as a plug flow reactor for which the radial mass transfer resistance is represented by a fictitious stagnant layer. For the higher range of velocities, the departure from ideality such as concentration gradients in the axial direction can be handled by extending the PFR to the axial dispersion model.

In the latter, we refer to microreactors which can be modeled accurately due to the well-defined underlying physics and geometry. The characteristic dimensions ensure a parabolic velocity profile and a homogeneous light intensity across the surface of the reactor. For these reasons microreactors with an immobilized porous layer of photocatalyst on one or both of the channel walls, are attractive devices to obtain the intrinsic kinetics.[20] As described previously, for immobilized layers scattering can be neglected (see the radiative transfer section).

Light-dependent kinetics can be derived for intrinsic semiconductors based on their fundamental physics.[18] For the diffusion-reaction regime, light-dependent kinetics can also be tackled analytically. Furthermore, a corresponding internal effectiveness factor has been derived[20] which is evaluating the catalyst coverage by taking into account both mass and radiative transfer limitations:

$$\eta = \frac{-1}{\delta}\frac{I_1\left(\frac{2\phi\sqrt{e^{-\gamma\alpha\delta}}}{\gamma\alpha\delta}\right)K_1\left(\frac{2\phi}{\gamma\alpha\delta}\right) - K_1\left(\frac{2\phi\sqrt{e^{-\gamma\alpha\delta}}}{\gamma\alpha}\right)I_1\left(\frac{2\phi}{\gamma\alpha\delta}\right)}{I_0\left(\frac{2\phi}{\gamma\alpha\delta}\right)K_1\left(\frac{2\phi\sqrt{e^{-\gamma\alpha\delta}}}{\gamma\alpha\delta}\right) + K_0\left(\frac{2\phi}{\gamma\alpha\delta}\right)I_1\left(\frac{2\phi\sqrt{e^{-\gamma\alpha\delta}}}{\gamma\alpha\delta}\right)} \tag{17}$$

where a modified Thiele modulus was computed as the ratio between surface reaction rate and the diffusion rate:

$$\phi^2 = \frac{k_i\delta^2}{D_{\text{eff}}}\left(\frac{\alpha\Phi_0}{Bp_0n_0\hbar\omega}\right)^{\gamma} \tag{18}$$

where $Bp_0n_0 \cong 3.3 \times 10^{-23}$ m^{-3} s^{-1} is the equilibrium electron−hole recombination rate.[18] $I_n(x)$ and $K_n(x)$ are modified Bessel functions of the first and second kind, respectively.

CONCLUSIONS

In this review, we tackle the underlying physics of photocatalytic reactions by providing rational reasoning for simplified analytic descriptions. We begin by analyzing the charge carrier generation and transfer, move on to radiative transfer based on the distribution and properties of the catalytic material, and account for the mass transfer both inside and outside the porous structure. Finally, we discuss the consequences for the most basic reactor designs for which guidelines and criteria are provided to meet their assumptions.

For ideal intrinsic semiconductors, the photocatalytic reaction rate scales linearly with light intensity if mass transfer is accurately accounted for. Simplifications to the radiative transfer equation should start based on a physical under-

DOI: 10.1021/acs.iecr.9b00381
Ind. Eng. Chem. Res. 2019, 58, 5349−5357

standing of the scattering angular dependency on the size of the particles with respect to the wavelength. The particle size regime can also give an idea about the scattering magnitude. It is only in the framework of pertinent assumptions that the experimental measurements can be correctly interpreted to provide true optical properties. The validity of simpler models, such as exponential attenuation of light, could be confirmed for a certain particle density regime by testing the proportionality between particle concentration and light attenuation. Immobilized films benefit from negligible scattering with simple transmission measurements revealing true absorption coefficients that can be used in dispersed systems to decouple absorption from scattering. The reaction-driven regime should be established using criteria such as the Thiele modulus, the internal effectiveness factor and Carberry criterion or mass transport limitations should be properly described using for example the stagnant boundary layer model or the axial dispersion model. Empirical tests are also presented to discard both external and internal mass transfer limitations.

This review should be of assistance in designing experiments for which the underlying assumptions for various photocatalytic models are accurately met and reveal the operating condition range for which these values are still accurate. Those who deal with rigorous 3D computational modeling can foresee the possible complexities for certain creative designs that may venture outside the experimental data set and care can be exercised when trying to extrapolate. Having a good grasp of the intricacies of the system, they can identify the missing parameters and establish a dialogue with experimentalists. This will aid in creating a situation in which the experimental endeavors are directed purposefully by investigating better defined questions from researchers in complementary fields.

AUTHOR INFORMATION

Corresponding Author

*E-mail: r.g.h.lammertink@utwente.nl. Tel.: +31 (0) 534892063.

ORCID

J. Ruud van Ommen: 0000-0001-7884-0323

Rob G. H. Lammertink: 0000-0002-0827-2946

Notes

The authors declare no competing financial interest.

ACKNOWLEDGMENTS

This work was supported by The Netherlands Center for Multiscale Catalytic Energy Conversion (MCEC), an NWO Gravitation programme funded by the Ministry of Education, Culture and Science of the government of The Netherlands. This contribution was identified by Jimmy A. Faria (University of Twente) and M. F. Neira D'Angelo (Eindhoven University of Technology) as the Best Presentation in the "Water (The Greenest Solvent): Catalysis in Aqueous & Bi-Phase Systems" session of the 2018 ACS Fall National Meeting in Boston.

REFERENCES

(1) Van Gerven, T.; Mul, G.; Moulijn, J.; Stankiewicz, A. A Review of Intensification of Photocatalytic Processes. *Chem. Eng. Process.* **2007**, *46*, 781−789.

(2) Arancibia-Bulnes, C. A.; Jiménez, A. E.; Estrada, C. A. Development and Modeling of Solar Photocatalytic Reactors. *Adv. Chem. Eng.* **2009**, *36*, 185−227.

(3) Ni, M.; Leung, M. K.; Leung, D. Y.; Sumathy, K. A Review and Recent Developments in Photocatalytic Water-splitting using TiO2 for Hydrogen Production. *Renewable Sustainable Energy Rev.* **2007**, *11*, 401−425.

(4) Lam, S. W.; Chiang, K.; Lim, T. M.; Amal, R.; Low, G. K. The Effect of Platinum and Silver Deposits in the Photocatalytic Oxidation of Resorcinol. *Appl. Catal., B* **2007**, *72*, 363−372.

(5) van Ommen, J. R.; Kooijman, D.; de Niet, M.; Talebi, M.; Goulas, A. Continuous Production of Nanostructured Particles using Spatial Atomic Layer Deposition. *J. Vac. Sci. Technol., A* **2015**, *33*, 021513.

(6) Teoh, W. Y.; Scott, J. A.; Amal, R. Progress in Heterogeneous Photocatalysis: From Classical Radical Chemistry to Engineering Nanomaterials and Solar Reactors. *J. Phys. Chem. Lett.* **2012**, *3*, 629−639.

(7) Ikeda, S.; Sugiyama, N.; Pal, B.; Marcí, G.; Palmisano, L.; Noguchi, H.; Uosaki, K.; Ohtani, B. Photocatalytic Activity of Transition-metal-loaded Titanium(IV) Oxide Powders Suspended in Aqueous Solutions: Correlation with Electron-hole Recombination Kinetics. *Phys. Chem. Chem. Phys.* **2001**, *3*, 267−273.

(8) Malato, S.; Fernández-Ibáñez, P.; Maldonado, M. I.; Blanco, J.; Gernjak, W. Decontamination and Disinfection of Water by Solar Photocatalysis: Recent Overview and Trends. *Catal. Today* **2009**, *147*, 1−59.

(9) Testino, A.; Bellobono, I. R.; Buscaglia, V.; Canevali, C.; D'Arienzo, M.; Polizzi, S.; Scotti, R.; Morazzoni, F. Optimizing the Photocatalytic Properties of Hydrothermal TiO2 by the Control of Phase Composition and Particle Morphology. A Systematic Approach. *J. Am. Chem. Soc.* **2007**, *129*, 3564−3575.

(10) Wang, C. C.; Zhang, Z.; Ying, J. Y. Photocatalytic Decomposition of Halogenated Organics over Nanocrystalline Titania. *Nanostruct. Mater.* **1997**, *9*, 583−586.

(11) Zhang, Z.; Wang, C.-C.; Zakaria, R.; Ying, J. Y. Role of Particle Size in Nanocrystalline TiO 2 -Based Photocatalysts. *J. Phys. Chem. B* **1998**, *102*, 10871−10878.

(12) Herrmann, J. M. Heterogeneous Photocatalysis: Fundamentals and Applications to the Removal of Various Types of Aqueous Pollutants. *Catal. Today* **1999**, *53*, 115−129.

(13) Hoffmann, M. R.; Martin, S. T.; Choi, W.; Bahnemann, D. W. Environmental Applications of Semiconductor Photocatalysis. *Chem. Rev.* **1995**, *95*, 69−96.

(14) Ollis, D. F. Photocatalytic Purification and Remediation of Contaminated Air and Water. *C. R. Acad. Sci., Ser. IIc: Chim.* **2000**, *3*, 405−411.

(15) Turchi, C. S.; Ollis, D. F. Photocatalytic Degradation of Organic Water Contaminants: Mechanisms involving Hydroxyl Radical attack. *J. Catal.* **1990**, *122*, 178−192.

(16) Motegh, M.; Cen, J.; Appel, P. W.; van Ommen, J. R.; Kreutzer, M. T. Photocatalytic-reactor Efficiencies and Simplified Expressions to assess their Relevance in Kinetic Experiments. *Chem. Eng. J.* **2012**, *207−208*, 607−615.

(17) Demeestere, K.; Visscher, A. D.; Dewulf, J.; van Leeuwen, M.; van Langenhove, H. A new Kinetic Model for Titanium Dioxide mediated Heterogeneous Photocatalytic Degradation of Trichloroethylene in Gas-phase. *Appl. Catal., B* **2004**, *54*, 261−274.

(18) Nielsen, M. G.; In, S. I.; Vesborg, P. C.; Pedersen, T.; Almtoft, K. P.; Andersen, I. H.; Hansen, O.; Chorkendorff, I. A Generic Model for Photocatalytic Activity as a Function of Catalyst Thickness. *J. Catal.* **2012**, *289*, 62−72.

(19) Colbeau-Justin, C.; Valenzuela, M. A. Time-resolved Microwave Conductivity (TRMC) a useful Characterization Tool for Charge Carrier Transfer in Photocatalysis: A Short Review. *Rev. Mex. Fis.* **2013**, *59*, 191−200.

(20) Visan, A.; Rafieian, D.; Ogieglo, W.; Lammertink, R. G. H. Modeling Intrinsic Kinetics in Immobilized Photocatalytic Microreactors. *Appl. Catal., B* **2014**, *150−151*, 93−100.

(21) Thiele, E. S.; French, R. H. Light-Scattering Properties of Representative, Morphological Rutile Titania Particles Studied Using a Finite-Element Method. *J. Am. Ceram. Soc.* **1998**, *81*, 469−479.

DOI: 10.1021/acs.iecr.9b00381
Ind. Eng. Chem. Res. 2019, 58, 5349−5357

(22) Ripoll, J. Derivation of the Scalar Radiative Transfer Equation from Energy Conservation of Maxwell's Equations in the Far Field. *J. Opt. Soc. Am. A* **2011**, *28*, 1765.
(23) Brandi, R. J.; Alfano, O. M.; Cassano, A. E. Modeling of Radiation Absorption in a Flat Plate Photocatalytic Reactor. *Chem. Eng. Sci.* **1996**, *51*, 3169−3174.
(24) Cabrera, M. I.; Alfano, O. M.; Cassano, A. E. Absorption and Scattering Coefficients of Titanium Dioxide Particulate Suspensions in Water. *J. Phys. Chem.* **1996**, *100*, 20043−20050.
(25) Cassano, A. E.; Alfano, O. M. Reaction Engineering of Suspended Solid Heterogeneous Photocatalytic Reactors. *Catal. Today* **2000**, *58*, 167−197.
(26) Spadoni, G.; Bandini, E.; Santarelli, F. Scattering Effects in Photosensitized Reactions. *Chem. Eng. Sci.* **1978**, *33*, 517−524.
(27) Domínguez-Arvizu, J. L.; Jiménez-Miramontes, J. A.; Salinas-Gutiérrez, J. M.; Meléndez-Zaragoza, M. J.; López-Ortiz, A.; Collins-Martínez, V. Study of NiFe2O4 Nanoparticles Optical Properties by a Six-flux Radiation Model towards the Photocatalytic Hydrogen Production. *Int. J. Hydrogen Energy* **2018**, 1−8.
(28) Mueses, M. A.; Machuca-Martinez, F.; Hernández-Ramirez, A.; Li Puma, G. Effective Radiation Field Model to Scattering - Absorption applied in Heterogeneous Photocatalytic Reactors. *Chem. Eng. J.* **2015**, *279*, 442−451.
(29) Orozco, S. L.; Villafán-Vidales, H. I.; Arancibia-Bulnes, C. A. Photon Absorption in a Hybrid Slurry Photocatalytic Reactor: Assessment of Differential Approximations. *AIChE J.* **2012**, *58*, 3256−3265.
(30) Li Puma, G.; Brucato, A. Dimensionless Analysis of Slurry Photocatalytic Reactors using Two-flux and Six-flux Radiation Absorption-scattering Models. *Catal. Today* **2007**, *122*, 78−90.
(31) Brucato, A.; Rizzuti, L. Simplified Modeling of Radiant Fields in Heterogeneous Photoreactors. 2. Limiting "Two-Flux" Model for the Case of Reflectance Greater Than Zero. *Ind. Eng. Chem. Res.* **1997**, *36*, 4748−4755.
(32) Li Puma, G. Modeling of Thin-Film Slurry Photocatalytic Reactors Affected by Radiation Scattering. *Environ. Sci. Technol.* **2003**, *37*, 5783−5791.
(33) Motegh, M.; van Ommen, J. R.; Appel, P. W.; Mudde, R. F.; Kreutzer, M. T. Bubbles Scatter Light, yet that does not hurt the Performance of Bubbly Slurry Photocatalytic Reactors. *Chem. Eng. Sci.* **2013**, *100*, 506−514.
(34) Turolla, A.; Santoro, D.; de Bruyn, J. R.; Crapulli, F.; Antonelli, M. Nanoparticle Scattering Characterization and Mechanistic Modelling of UV-TiO2 Photocatalytic Reactors using Computational Fluid Dynamics. *Water Res.* **2016**, *88*, 117−126.
(35) Acosta-Herazo, R.; Monterroza-Romero, J.; Mueses, M. Á.; Machuca-Martínez, F.; Li Puma, G. Coupling the Six Flux Absorption-Scattering Model to the Henyey-Greenstein Scattering Phase Function: Evaluation and Optimization of Radiation Absorption in Solar Heterogeneous Photoreactors. *Chem. Eng. J.* **2016**, *302*, 86−96.
(36) Satuf, M. L.; Brandi, R. J.; Cassano, A. E.; Alfano, O. M. Experimental Method to Evaluate the Optical Properties of Aqueous Titanium Dioxide Suspensions. *Ind. Eng. Chem. Res.* **2005**, *44*, 6643−6649.
(37) Moreira, J.; Serrano, B.; Ortiz, A.; de Lasa, H. TiO2 Absorption and Scattering Coefficients using Monte Carlo Method and Macroscopic Balances in a Photo-CREC Unit. *Chem. Eng. Sci.* **2011**, *66*, 5813−5821.
(38) Valades-Pelayo, P. J.; Moreira, J.; Serrano, B.; De Lasa, H. Boundary Conditions and Phase Functions in a Photo-crec Water-II Reactor Radiation Field. *Chem. Eng. Sci.* **2014**, *107*, 123−136.
(39) Bohren, C. F.; Huffman, D. R. *Absorption and Scattering of Light by Small Particles*; Wiley-VCH Verlag GmbH: Weinheim, Germany, 2015; Vol. *35*; pp 104−104.
(40) Diebold, M. P. *Appl. Light Scatt. to Coatings*; Springer International Publishing: Cham, 2014.
(41) van de Hulst, H. C. *Light Scattering by Small Particles*; Dover Publications Inc.: New York, 1981.
(42) Rafieian, D.; Driessen, R. T.; Ogieglo, W.; Lammertink, R. G. H. Intrinsic Photocatalytic Assessment of Reactively Sputtered TiO2 Films. *ACS Appl. Mater. Interfaces* **2015**, *7*, 8727−8732.
(43) Butt, J. B. *Reaction Kinetics and Reactor Design*, Prentice-Hall, Inc.: Engelwood Cliffs, New Jersey, 1980.
(44) Morbidelli, M.; Varma, A.; Aris, R. *Chemical Reaction and Reactor Engineering*; CRC Press: 1987; pp 973−1054.
(45) Mehrotra, K.; Yablonsky, G. S.; Ray, A. K. Macro Kinetic Studies for Photocatalytic Degradation of Benzoic Acid in Immobilized Systems. *Chemosphere* **2005**, *60*, 1427−1436.
(46) Assadi, A. A.; Bouzaza, A.; Wolbert, D. Photocatalytic Oxidation of Trimethylamine and Isovaleraldehyde in an Annular Reactor: Influence of the Mass Transfer and the Relative Humidity. *J. Photochem. Photobiol., A* **2012**, *236*, 61−69.
(47) McEligoi, D. Fundamentals of momentum, heat and mass transfer. *Int. J. Heat Mass Transfer* **1970**, *13*, 1641.
(48) Levenspiel, O. *Chemical Reaction Engineering*, John Wiley and Sons, 1998.
(49) Nur, Y.; Lead, J.; Baalousha, M. Evaluation of Charge and Agglomeration Behavior of TiO2 Nanoparticles in Ecotoxicological Media. *Sci. Total Environ.* **2015**, *535*, 45−53.

DOI: 10.1021/acs.iecr.9b00381
Ind. Eng. Chem. Res. 2019, 58, 5349−5357